

# Fine-Tuning the Energy Barrier for Metal-Mediated Dinitrogen $\text{N}\equiv\text{N}$ Bond Cleavage

Andrew J. Keane, Brendan L. Yonke, Masakazu Hirotsu, Peter Y. Zavalij, and Lawrence R. Sita\*

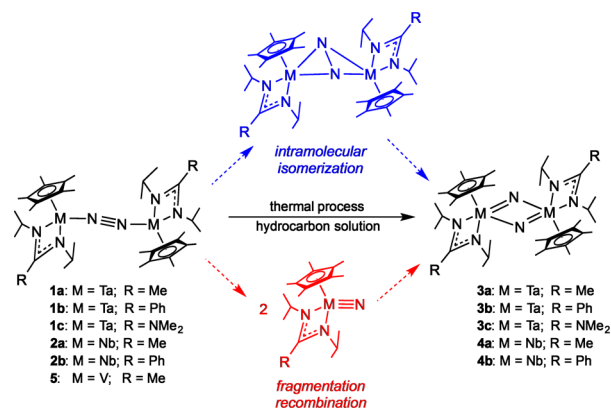
Department of Chemistry and Biochemistry, University of Maryland, College Park, Maryland 20742, United States

**S** Supporting Information

**ABSTRACT:** Experimental data support a mechanism for  $\text{N}\equiv\text{N}$  bond cleavage within a series of group 5 bimetallic dinitrogen complexes of general formula,  $\{\text{Cp}^*\text{M}[\text{N}(\text{iPr})\text{C}(\text{R})\text{N}(\text{iPr})]\}_2(\mu\text{-N}_2)$  ( $\text{Cp}^* = \eta^5\text{-C}_5\text{Me}_5$ ) ( $\text{M} = \text{Nb, Ta}$ ), that proceeds in solution through an intramolecular “end-on-bridged” ( $\mu\text{-}\eta^1:\eta^1\text{-N}_2$ ) to “side-on-bridged” ( $\mu\text{-}\eta^2:\eta^2\text{-N}_2$ ) isomerization process to quantitatively provide the corresponding bimetallic bis( $\mu$ -nitrido) complexes,  $\{\text{Cp}^*\text{M}[\text{N}(\text{iPr})\text{C}(\text{R})\text{N}(\text{iPr})](\mu\text{-N})\}_2$ . It is further demonstrated that subtle changes in the steric and electronic features of the distal R-substituent, where  $\text{R} = \text{Me, Ph}$  and  $\text{NMe}_2$ , can serve to modulate the magnitude of the free energy barrier height for  $\text{N}\equiv\text{N}$  bond cleavage as assessed by kinetic studies and experimentally derived activation parameters. The origin of the contrasting kinetic stability of the first-row congener,  $\{\text{Cp}^*\text{V}[\text{N}(\text{iPr})\text{C}(\text{Me})\text{N}(\text{iPr})]\}_2(\mu\text{-}\eta^1:\eta^1\text{-N}_2)$  toward  $\text{N}\equiv\text{N}$  bond cleavage is rationalized in terms of a ground-state electronic structure that favors a significantly less-reduced  $\mu\text{-N}_2$  fragment.

A central requirement of nitrogen fixation, which encompasses all chemical and biochemical processes that convert molecular dinitrogen ( $\text{N}_2$ ) into more reduced nitrogen-containing products, and most essentially, ammonia ( $\text{NH}_3$ ), is a reaction pathway that can ultimately surmount the high free energy barrier associated with breaking the exceptionally strong  $\text{N}\equiv\text{N}$  triple bond.<sup>1–4</sup> Many seminal advances have been made over the past 100 years with delineating the mechanisms of different metal-mediated nitrogen fixation schemes. However, to date, no experimental system has yet been discovered or devised—whether of chemical or biochemical inspiration—that permits one to systematically probe the impact of changes in molecular and electronic structure on the free energy barrier height of a well-established  $\text{N}\equiv\text{N}$  bond cleaving process through the programmed synthesis of a family of substitutionally differentiated derivatives. Herein, we now present such a system that is based on the thermal conversion of group 5 bimetallic dinitrogen complexes of general formula,  $\{\text{Cp}^*\text{M}[\text{N}(\text{iPr})\text{C}(\text{R})\text{N}(\text{iPr})]\}_2(\mu\text{-N}_2)$  ( $\text{Cp}^* = \eta^5\text{-C}_5\text{Me}_5$ ), where  $\text{M} = \text{Ta}$  (**1**) and  $\text{Nb}$  (**2**), to the corresponding bimetallic bis( $\mu$ -nitrido) complexes,  $\{\text{Cp}^*\text{M}[\text{N}(\text{iPr})\text{C}(\text{R})\text{N}(\text{iPr})](\mu\text{-N})\}_2$ , where  $\text{M} = \text{Ta}$  (**3**) and  $\text{Nb}$  (**4**), respectively, according to Scheme 1.<sup>5</sup> Importantly, through synthetic manipulation of the steric and electronic nature of the distal R-substituent of **1** and **2**, and specifically, where  $\text{R} = \text{Me}$  (**a**),  $\text{Ph}$  (**b**) and  $\text{NMe}_2$  (**c**), we provide experimental data in support of an intramolecular  $\mu\text{-}\eta^1:\eta^1\text{-N}_2 \rightarrow \mu\text{-}\eta^2:\eta^2\text{-N}_2$  isomer-

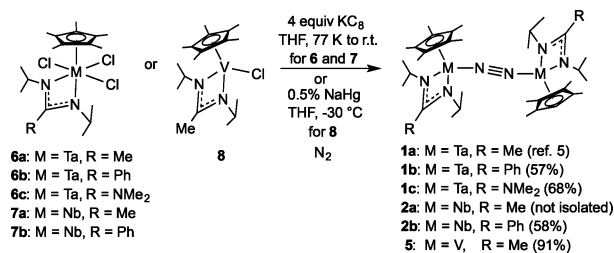
Scheme 1



ization process as the most likely pathway involved, rather than the alternative of initial homolytic  $\text{N}\equiv\text{N}$  bond fragmentation to a transient terminal nitride species followed by bimolecular recombination (cf. upper and lower paths of Scheme 1, respectively). Finally, we establish that the sharply contrasting kinetic stability of the first-row congener,  $\{\text{Cp}^*\text{V}[\text{N}(\text{iPr})\text{C}(\text{Me})\text{N}(\text{iPr})]\}_2(\mu\text{-N}_2)$  (**5**), is most likely the consequence of a change in the ground-state electronic structure of this bimetallic dinitrogen complex that favors more reduced metal centers and a less-reduced central  $\mu\text{-N}_2$  fragment.<sup>4</sup>

In 2007, we reported that the ditantalum “end-on-bridged” dinitrogen complex **1a** could be isolated as a paramagnetic crystalline material through chemical reduction of the tantalum trichloride,  $\text{Cp}^*\text{M}[\text{N}(\text{iPr})\text{C}(\text{R})\text{N}(\text{iPr})]\text{Cl}_3$ , where  $\text{M} = \text{Ta}$  and  $\text{R} = \text{Me}$  (**6a**), in tetrahydrofuran (THF) solution at low temperature using 4 equiv of potassium graphite ( $\text{KC}_8$ ) as the reductant according to Scheme 2.<sup>5–7</sup> In hydrocarbon (e.g.,

Scheme 2



Received: May 27, 2014

Published: June 24, 2014

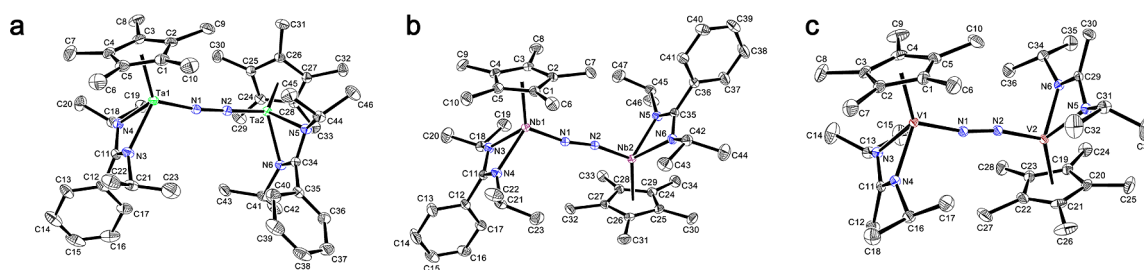


**Figure 1.** Molecular structures (30% thermal ellipsoids) of (a) **1b**, (b) **2b** and (c) **5**. Hydrogen atoms have been removed for the sake of clarity.<sup>8</sup>

toluene or pentane) solution, pure samples of **1a** were observed to quantitatively convert to the ditantalum bis( $\mu$ -nitrido) complex **3a** at temperatures above 0 °C according to Scheme 1.

In the present work, similar  $\text{KC}_8$  reductions of the trichlorides **6b** and **6c**, where  $\text{R} = \text{Ph}$  and  $\text{NMe}_2$ , respectively, provided the corresponding complexes **1b** and **1c** in good yields.<sup>8</sup> Interestingly, both of these derivatives proved to be more kinetically stable in solution at room temperature than **1a** (*vide infra*). Upon moving to the second row, chemical reduction of the niobium trichloride **7a** (see Scheme 2) in standard fashion now provided a green-colored solution that only persisted at temperatures below  $-30$  °C. Upon warming to room temperature, this same solution rapidly turned pale-orange in color, and after the typical workup, no trace of the desired dinitrogen complex **2a** could be obtained, but rather, only the bis( $\mu$ -nitrido) product **4a** was isolated (see Scheme 1).<sup>8</sup> However, similar to the increased stability of **1b** *vis-à-vis* **1a**, chemical reduction of the niobium trichloride **7b** ( $\text{R} = \text{Ph}$ ) now provided the paramagnetic dinioium dinitrogen complex **4b** (58% yield) that likewise displayed good kinetic stability in solution at 0 °C. Finally, to complete an entire group 5 isostructural series, chemical reduction of  $\text{Cp}^*\text{V}[\text{N}(\text{Pr})\text{C}(\text{Me})\text{N}(\text{Pr})\text{Cl}]$  (**8**), but now using 0.5% sodium amalgam ( $\text{NaHg}$ ) as the reductant in THF at  $-30$  °C, produced an excellent 91% yield of the paramagnetic divanadium dinitrogen complex **5** that surprisingly proved to be thermally robust in solution up to temperatures of 90 °C.<sup>8</sup> It can be further noted that, except for  $\text{M} = \text{Cr}$ , synthetic derivatives of  $\{\text{Cp}^*\text{M}[\text{N}(\text{Pr})\text{C}(\text{R})\text{N}(\text{Pr})]\}_2(\mu\text{-N}_2)$  have now been prepared for the entire set of groups 4–6 metals ( $\text{M} = \text{Ti}$ ,<sup>7</sup>  $\text{Zr}$ ,<sup>6</sup>  $\text{Hf}$ ,<sup>6</sup>  $\text{V}$ ,  $\text{Nb}$ ,  $\text{Ta}$ ,<sup>5</sup>  $\text{Mo}$ ,<sup>7</sup> and  $\text{W}$ <sup>7</sup>).

Analytical characterization data for the new group 5 bimetallic dinitrogen complexes **1b**, **1c**, **2b**, and **5** were consistent with the expected empirical formulas, and single crystal X-ray analyses served to establish the  $\mu\text{-}\eta^1\text{-}\eta^1\text{-N}_2$  coordination motif in the solid state according to the structural data presented in Figure 1. Of particular interest are the relative magnitudes of the nitrogen–nitrogen bond distances  $d(\text{NN})$  as a function of the metal row number. In this respect, the values displayed by the second- and third-row derivatives of **1** and **2** are consistent with a strong degree of  $\text{N}\equiv\text{N}$  bond activation and a formal  $[\text{M}(\text{IV}), d^1, \text{M}(\text{IV}), d^1]$  ( $\text{M} = \text{Nb}, \text{Ta}$ ) open-shell electronic ground state, whereas those for the first row analog **5** are more in keeping with a much smaller degree of  $\text{N}_2$  activation and more reduced metal centers, such as a formal  $[\text{V}(\text{II}), d^3, \text{V}(\text{II}), d^3]$  electronic structure, [cf. **1a**:  $d(\text{NN}) = 1.313(4)$  Å; **1b**:  $1.308(5)$  Å; **1c**:  $1.306(5)$  Å; **2b**:  $1.300(3)$  Å; **5**:  $1.225(2)$  Å].<sup>4,5,7,9</sup>

As already previously noted, derivatives of **1** and **2** exhibited profound differences in kinetic stability in solution depending upon the nature of the distal R-substituent, and qualitatively, in order of decreasing stability for  $\text{R} = \text{Ph} > \text{NMe}_2 > \text{Me}$ . Further, in keeping with the original observation of **1a** quantitatively

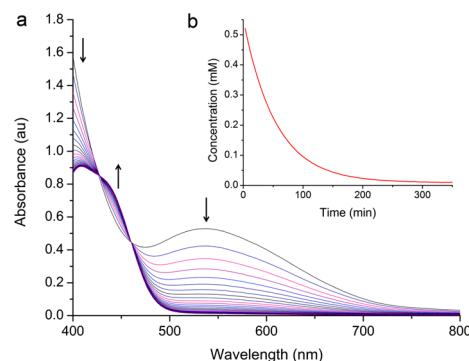


**Figure 2.** (a) Scanning UV–vis spectroscopy for  $(^{15}\text{N}_2, 98\%)\text{-1a} \rightarrow (^{15}\text{N}_2, 98\%)\text{-3a}$  at  $T = 318.15$  K.<sup>8</sup> (b) Kinetic analysis of  $[\mathbf{1a}]_t$  vs time as monitored at  $\lambda = 625$  nm.

converting to a *cis*, *trans* isomeric mixture of **3a**, bulk thermolysis in hydrocarbon solutions of **1b**, **1c**, and **2b** provided excellent isolated yields of the corresponding diamagnetic bimetallic bis( $\mu$ -nitrido) complexes **3b**, **3c**, and **4b**, respectively, as crystalline mixtures. Fractional crystallization and single-crystal X-ray analysis then confirmed the structural identity of either a *trans* or *cis* isomer in each case, along with solid-state geometric parameters that confirmed the absence of N–N bonding [cf. calculated  $d(\text{NN})$  values  $>2.55$  Å].<sup>8</sup>

Detailed kinetic investigations of the thermal conversions presented in Scheme 1 were conducted for methylcyclohexane solutions using variable-temperature scanning UV–vis spectroscopy.<sup>8</sup> Figure 2a presents typical data obtained at a given temperature by this method that further confirmed the quantitative nature of each thermal reaction through the appearance of sharply focused isosbestic points in an overlay plot of spectra collected at fixed time intervals. By monitoring the rate of disappearance of the bimetallic dinitrogen complex as a function of time at a single fixed wavelength (see Figure 2b), kinetic rate data at five different temperatures (in triplicate) over a temperature range (cf. 313–333 K for **1a** and **2b**, 328–353 K for **1c**, and 343–368 K for **1b**) were collected and fit to the Eyring equation as shown in Figure 3, and from which, the set of activation parameters provided in Table 1 were derived.<sup>8</sup> Further studies revealed that kinetic parameters remained invariant over a range of concentrations and that initial rates were consistent with being first-order in dinitrogen complex. Finally, kinetic analysis of the thermal conversion of isotopically labeled  $(^{15}\text{N}_2, 98\%)\text{-1a}$  to  $(^{15}\text{N}_2, 98\%)\text{-3a}$  was performed in similar fashion (see Table 1).

Based on the experimentally derived enthalpic and entropic activation parameters,  $\Delta H^\ddagger$  and  $\Delta S^\ddagger$ , respectively, of Table 1,  $\Delta G^\ddagger$  values were computed for the fixed temperature of 338.15 K and these were found to be consistent with the observed trend in thermal stability of **1b** ( $\text{R} = \text{Ph}$ )  $>$  **1c** ( $\text{NMe}_2$ )  $>$  **1a** ( $\text{Me}$ ). A comparison of the kinetic data and activation parameters for the

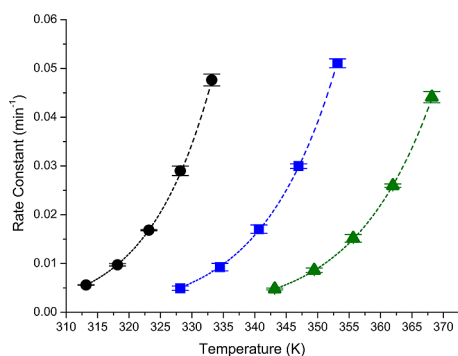


**Figure 3.** Temperature-dependent first-order rate constants with least-squares fit to the Eyring equation,  $k = (k_B T/h) \exp(\Delta S^\ddagger/R) \exp(-\Delta H^\ddagger/RT)$ , for the conversion of **1a**  $\rightarrow$  **3a** (circle), **1c**  $\rightarrow$  **3c** (square) and **1b**  $\rightarrow$  **3b** (triangle). For a similar analysis of data for the conversion of **2b**  $\rightarrow$  **4b**, see Supporting Information.<sup>8</sup>

**Table 1. Experimentally-Derived Activation Parameters for Thermal Conversion of 1  $\rightarrow$  3 and 2b  $\rightarrow$  4b**

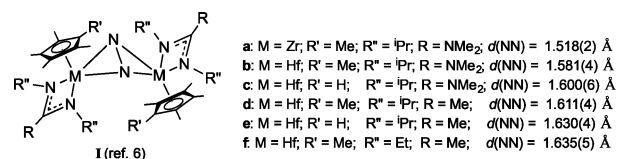
	$\Delta G^\ddagger$ (kcal/mol) <sup>a,b</sup>	$\Delta H^\ddagger$ (kcal/mol) <sup>b</sup>	$\Delta S^\ddagger$ (cal/(mol K)) <sup>b</sup>
<b>1a</b>	24.3(3)	21.5(3)	-8.4(9)
<b>1a</b> ( <sup>15</sup> N <sub>2</sub> )	24.4(2)	21.8(2)	-7.4(6)
<b>1c</b>	25.5(3)	20.6(3)	-14.6(8)
<b>1b</b>	26.6(3)	21.7(3)	-14.4(8)
<b>2b</b>	24.4(1)	20.2(1)	-12.4(5)

<sup>a</sup>Calculated at 338.15 K. <sup>b</sup>Error reported at the 95% confidence interval.

second-row derivative **2b** (R = Ph) reveals that it is similar in stability to **1a** [cf.  $\Delta G^\ddagger$  (338.15 K) = 24.3(3) kcal mol<sup>-1</sup> for **1a** vs 24.4(1) kcal mol<sup>-1</sup> for **2b**] (see Table 1).<sup>8</sup> Intriguingly, all  $\Delta S^\ddagger$  values are negative in magnitude, which implies a more highly ordered transition state that must be reached for the rate-determining step along the reaction pathway. Indeed, as Table 1 reveals, the greatest contributing factor for the increase in  $\Delta G^\ddagger$  values in the order of **1a** < **1c** < **1b** is the large 6 cal mol<sup>-1</sup> K<sup>-1</sup> negative change in  $\Delta S^\ddagger$  associated with the more sterically encumbered R = Ph and NMe<sub>2</sub> substituents of **1b** and **1c**, respectively, relative to R = Me for **1a**. In analyzing data for the former pair more closely, the notable difference in the enthalpic term [cf.  $\Delta H^\ddagger$  = 20.6(3) kcal mol<sup>-1</sup> for **1c** vs 21.7(3) kcal mol<sup>-1</sup> for **1b**] might suggest more stabilization of the formally oxidized metal centers of the transition state by the electron-rich NMe<sub>2</sub> substituent relative to the Ph group. Finally, in comparing the second- and third-row derivatives bearing the same R = Ph substituent, it is notable from the data of Table 1 that the much smaller calculated  $\Delta G^\ddagger$  (338.15 K) value of 24.4(1) kcal mol<sup>-1</sup> obtained for **2b** relative to that of **1b** at 26.6(3) kcal mol<sup>-1</sup> is largely due to a significant reduction in the change in enthalpy of activation term,  $\Delta H^\ddagger$ , which is 20.2(1) kcal mol<sup>-1</sup> for **2b** vs 21.7(3) kcal mol<sup>-1</sup> for **1b**. In summary, these kinetic data strongly suggest that, at least for the present supporting ligand environment, diniobium  $\mu$ - $\eta^1$ : $\eta^1$ -N<sub>2</sub> complexes will possess an intrinsically lower potential energy barrier for N $\equiv$ N bond cleavage relative to a ditantalum  $\mu$ - $\eta^1$ : $\eta^1$ -N<sub>2</sub> congener and that a sterically demanding distal R-substituent is critical for kinetically stabilizing an isolable diniobium dinitrogen derivative.

Upon sodium metal reduction in dimethoxyethane (DME) solution, rearrangement of a diniobium end-on-bridged  $\mu$ - $\eta^1$ : $\eta^1$ -N<sub>2</sub> moiety to a diniobium side-on-bridged  $\mu$ - $\eta^2$ : $\eta^2$ -N<sub>2</sub> group that is stabilized by secondary sodium–nitrogen bonding interactions

**Chart 1**



within a structurally characterized reduced product has been reported by Floriani et al.<sup>10</sup> Fryzuk et al.<sup>11</sup> have also previously proposed that thermal conversion of a diniobium  $\mu$ - $\eta^1$ : $\eta^1$ -N<sub>2</sub> complex to a product arising from N $\equiv$ N bond cleavage and formal intramolecular insertion of a metal nitrido group into a niobium–phosphorus bond of the supporting ligand framework proceeds via a diniobium side-on-bridged  $\mu$ - $\eta^2$ : $\eta^2$ -N<sub>2</sub> intermediate. Although additional experimental support for such an intermediate or the proposed bimetallic  $\mu$ - $\eta^1$ : $\eta^1$ -N<sub>2</sub>  $\rightarrow$   $\mu$ - $\eta^2$ : $\eta^2$ -N<sub>2</sub> thermal rearrangement step was not provided, a computational investigation of the relative thermodynamic stabilities of simplified structural models for  $\mu$ - $\eta^1$ : $\eta^1$ -N<sub>2</sub> vs  $\mu$ - $\eta^2$ : $\eta^2$ -N<sub>2</sub> coordination appeared to put this hypothesis on firmer theoretical ground.<sup>12</sup> In our own studies, we have also previously stated that the most likely mechanism for thermal conversion of **1a** to **3a** involves an intramolecular  $\mu$ - $\eta^1$ : $\eta^1$ -N<sub>2</sub> to  $\mu$ - $\eta^2$ : $\eta^2$ -N<sub>2</sub> structural isomerization that occurs prior to N $\equiv$ N bond cleavage according to the upper pathway of Scheme 1.<sup>5,7</sup> The basis for this conjecture rested on structural data obtained for the set of related group 4 bimetallic dinitrogen derivatives,  $\{(\eta^5\text{-C}_5\text{Me}_4\text{R}')\text{M}[\text{N}(\text{R}'')\text{C}(\text{R})\text{N}(\text{R}'')]\}_2(\mu\text{-}\eta^2\text{:}\eta^2\text{-N}_2)$  (M = Zr and Hf) (**I**), which display exceedingly large  $d(\text{NN})$  values that increase as the magnitude of nonbonded steric interactions within the supporting ligand environment decrease as shown in Chart 1.<sup>6</sup> Due to the inability of the formal group 4 M(IV, d<sup>0</sup>) metal centers in these complexes to deliver any additional reducing electron equivalents to the central N $\equiv$ N bond, these structures can be viewed as representing “arrested” transition states for the proposed isomerization mechanism of Scheme 1.<sup>10</sup> More recently, Musaev et al.<sup>13</sup> have published the results of a detailed computational study of a simplified structural model for **1a**  $\rightarrow$  **3a** which provides additional theoretical support for our hypothesis.

As presented in the lower half of Scheme 1, a possible alternative mechanism for N $\equiv$ N bond cleavage within bimetallic end-on-bridged dinitrogen complexes is via homolytic N $\equiv$ N bond fragmentation to produce two equivalents of a metal terminal nitride product.<sup>4</sup> Experimental precedent for this pathway rests almost entirely with the seminal structural and kinetic studies performed by Cummins et al.<sup>14</sup> for the dimolybdenum dinitrogen complex,  $\{(\text{Ar}[\text{tBu}]\text{N})_3\text{Mo}\}_2(\mu\text{-}\eta^1\text{:}\eta^1\text{-N}_2)$  (Ar = 3,5-C<sub>6</sub>H<sub>3</sub>Me<sub>2</sub>) (**II**) that undergoes thermally induced N $\equiv$ N bond fragmentation to produce 2 equiv of the corresponding terminal metal nitride, (Ar[<sup>t</sup>Bu]N)<sub>3</sub>Mo(N) (**III**). Detailed kinetic and computational studies conducted by this group and others support a reaction profile that proceeds through a ‘trans-zigzag’ transition state leading to homolytic N $\equiv$ N bond cleavage and terminal metal nitride products.<sup>9,15</sup>

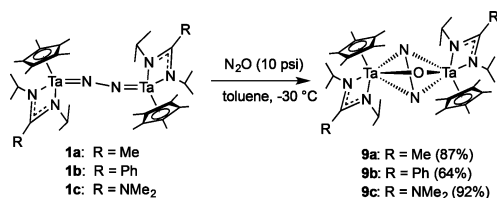
Since the magnitudes (i.e., negative  $\Delta S^\ddagger$ ) and trends in activation parameters presented in Table 1 do not unequivocally establish that an intramolecular isomerization mechanism is favored over homolytic N $\equiv$ N bond fragmentation for thermolysis of the present set of group 5 bimetallic dinitrogen complexes, several additional experimental results and lines of inquiry were pursued. Thus, to begin, comparing the



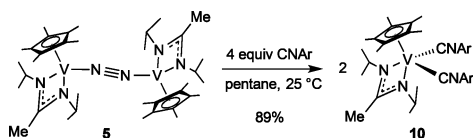
experimentally derived activation parameters obtained for  $^{15}\text{N}_2$  (98%)-labeled **1a** with those for unlabeled **1a** provided a very low to virtually nonexistent  $^{14}\text{N}_2/^{15}\text{N}_2$  kinetic isotope effect of 1.03(3) at 318.15 K, which would be consistent with an isomerization mechanism in which no significant  $\text{N}\equiv\text{N}$  bond cleavage had yet occurred in the transition state.<sup>14</sup> Second, a crossover experiment was conducted in which a concentrated solution consisting of a 1:1 mixture of **1a** and **1c** in THF, which was chosen as the solvent to maintain a homogeneous solution of starting materials and products, was heated to 70 °C for 3.5 h within a sealed tube. Analysis of the crude product mixture by electrospray ionization mass spectrometry subsequently revealed only the presence of parent molecular ions  $[\text{M} + \text{H}]^+$  at 943.21 and 1001.26  $m/z$  that correspond to **3a** and **3c**, respectively, and with no evidence being obtained for the theoretical crossover product,  $[\{\text{Cp}^*\text{Ta}[\text{N}(\text{iPr})\text{C}(\text{Me})\text{N}(\text{iPr})]\}\{\text{Cp}^*\text{Ta}[\text{N}(\text{iPr})\text{C}(\text{NMe}_2)\text{N}(\text{iPr})]\}\{\mu\text{-N}_2\}]$ , which would be expected to exhibit a molecular ion  $[\text{M} + \text{H}]^+$  at 972.45  $m/z$ . Finally, we undertook the synthesis of a comparable set of isolable ditantalum “side-on” dinitrogen complexes in which the magnitude of steric interactions within the supporting ligand environment remains approximately the same as **1**. Gratifyingly, introduction of nitrous oxide ( $\text{N}_2\text{O}$ ) into toluene solutions of **1a–c** at  $-30$  °C readily generated a new product in each case and in high yield that could be isolated as a diamagnetic, purple crystalline material.<sup>8</sup> As depicted in Scheme 3, analytic, spectroscopic, and single-crystal X-ray data served to establish the identity of these products as being,  $\{\text{Cp}^*\text{Ta}[\text{N}(\text{iPr})\text{C}(\text{R})\text{N}(\text{iPr})]\}_2(\mu\text{-}\eta^2\text{:}\eta^2\text{-N}_2)(\mu\text{-O})$  where  $\text{R} = \text{Me}$  (**9a**),  $\text{Ph}$  (**9b**), and  $\text{NMe}_2$  (**9c**).<sup>8</sup> Importantly, the latter structural data unequivocally confirm the ability of a  $[\text{Ta}(\text{V})$ ,  $\text{Ta}(\text{V})]$  dinitrogen complex to adopt side-on  $\mu\text{-N}_2$  coordination.<sup>16</sup> For all three structures, the unique  $\text{Ta}_2\text{N}_2$  fragment is characterized as being highly asymmetric with respect to  $d(\text{MN})$  values, and the  $d(\text{NN})$  parameter is large thereby suggesting a high degree of formal  $\text{N}\equiv\text{N}$  bond activation [cf. 1.493(12), 1.499(4), and 1.504(4) Å for **9a–c**, respectively].<sup>8</sup>

As a final consideration, we have begun to probe the possible origin(s) of the unique thermal solution stability displayed by the first-row divanadium dinitrogen complex **5** vis-à-vis that of **1** and **2**. Mendiola et al.<sup>9</sup> have previously explored the prohibitive kinetic barrier that exists for achieving  $\text{N}\equiv\text{N}$  bond cleavage within a  $[\text{V}(\text{II})$ ,  $\text{V}(\text{II})]$  ( $\mu\text{-}\eta^1\text{:}\eta^1\text{-N}_2$ ) complex. In the present study, the structural parameters obtained for **5** are highly suggestive of a similar ground-state electronic configuration, and

Scheme 3



Scheme 4



indeed, addition of 4 equiv of 2,6-dimethylphenylisocyanide to a pentane solution of **5** provided a 89% yield of the structurally characterized V(II) bis(isocyanide) complex,  $\text{Cp}^*\text{V}[\text{N}(\text{iPr})\text{C}(\text{Me})\text{N}(\text{iPr})]\{\text{CN}(2,6\text{-Me}_2\text{C}_6\text{H}_3)\}_2$  (**10**), according to Scheme 4.<sup>7,8</sup>

In summary, the present work serves to experimentally establish a thermal intramolecular pathway by which the exceptionally strong bond of  $\text{N}_2$  can be cleaved via bimetallic coordination and with external control over the free energy barrier.

## ASSOCIATED CONTENT

### Supporting Information

Experimental details and crystallographic analyses. This material is available free of charge via the Internet at <http://pubs.acs.org>.

## AUTHOR INFORMATION

### Corresponding Author

lsita@umd.edu

### Notes

The authors declare no competing financial interest.

## ACKNOWLEDGMENTS

Funding for this work was provided by the Department of Energy, Basic Energy Sciences (Grant DE-SC0002217) for which we are grateful.

## REFERENCES

- (1) Smil, V. *Enriching the Earth: Fritz Haber, Carl Bosch, and the Transformation of World Food Production*; MIT Press: Cambridge, MA, 2001.
- (2) (a) Howard, J. B.; Rees, D. C. *Proc. Natl. Acad. Sci. U.S.A.* **2006**, *103*, 17088. (b) Hu, Y.; Ribbe, M. W. *J. Biol. Inorg. Chem.* DOI: 10.1007/s00775-014-1137-2.
- (3) Ertl, G. *Catal. Rev. Sci. Eng.* **1980**, *21*, 201.
- (4) (a) Chirik, P. J. *Dalton Trans.* **2007**, 16. (b) Fryzuk, M. D. *Acc. Chem. Res.* **2009**, *42*, 127. (c) Tanabe, Y.; Nishibayashi, Y. *Coord. Chem. Rev.* **2013**, *257*, 2551.
- (5) Hirotsu, M.; Fontaine, P. P.; Epshteyn, A.; Zavalij, P. Y.; Sita, L. R. *J. Am. Chem. Soc.* **2007**, *129*, 9284.
- (6) Hirotsu, M.; Fontaine, P. P.; Zavalij, P. Y.; Sita, L. R. *J. Am. Chem. Soc.* **2007**, *129*, 12690.
- (7) Fontaine, P. P.; Yonke, B. L.; Zavalij, P. Y.; Sita, L. R. *J. Am. Chem. Soc.* **2010**, *132*, 12273.
- (8) Details are provided in the SI.
- (9) Tran, B. L.; Pinter, B.; Nichols, A. J.; Konopka, F. T.; Thompson, R.; Chen, C.-H.; Krzystek, J.; Ozarowski, A.; Telsler, J.; Baik, M.-H.; Meyer, K.; Mendiola, D. J. *J. Am. Chem. Soc.* **2012**, *134*, 13035.
- (10) Caselli, A.; Solari, E.; Scopelliti, R.; Floriani, C.; Re, N.; Rizzoli, C.; Chiesi-Villa, A. *J. Am. Chem. Soc.* **2000**, *122*, 3652.
- (11) Fryzuk, M. D.; Kozak, C. M.; Bowdridge, M. R.; Patrick, B. O.; Rettig, S. J. *J. Am. Chem. Soc.* **2002**, *124*, 8389.
- (12) Christian, G. J.; Terrett, R. N. L.; Stranger, R.; Cavigliasso, G.; Yates, B. F. *Chem.—Eur. J.* **2009**, *15*, 11373.
- (13) Zhang, W.; Tang, Y.; Lei, M.; Morokuma, K.; Musaev, D. G. *Inorg. Chem.* **2011**, *50*, 9481.
- (14) (a) Laplaza, C. E.; Cummins, C. C. *Science* **1995**, *268*, 861. (b) Laplaza, C. E.; Johnson, M. J. A.; Peters, J.; Odom, A. L.; Kim, E.; Cummins, C. C.; George, G. N.; Pickering, I. J. *J. Am. Chem. Soc.* **1996**, *118*, 8623. (c) Curley, J. J.; Cook, T. R.; Reece, S. Y.; Muller, P.; Cummins, C. C. *J. Am. Chem. Soc.* **2008**, *130*, 9394.
- (15) (a) Cui, Q.; Musaev, D. G.; Svensson, M.; Sieber, S.; Morokuma, K. *J. Am. Chem. Soc.* **1995**, *117*, 12366. (b) Brookes, N. J.; Graham, D. C.; Christian, G.; Stranger, R.; Yates, B. F. *J. Comput. Chem.* **2009**, *30*, 2146.
- (16) Fryzuk, M. D.; Johnson, S. A.; Rettig, S. J. *J. Am. Chem. Soc.* **1998**, *120*, 11024.